Int. j. adv. multidisc. res. stud. 2026; 6(3):1005-1011

Received: 12-04-2026
Accepted: 22-05-2026

International Journal of Advanced Multidisciplinary Research and Studies

ISSN: 2583-049X

Characterization and Physical Properties of Concrete Blocks Developed with Hongsa Fly Ash as a Cement Replacement

[1] Touypheng Vonsonethai, [2] Kongsy Phimmavong, [3] Phoutthamala Siththivong, [4] Pem Phakviseth

[1] Master Program, Organization Resources, Souphanouvong University, Luang Prabang Province, Lao PDR

[2, 4] Department of Material Science and Engineering, Faculty of Engineering, Souphanouvong University, Luang Prabang Province, Lao PDR

[3] Department of Civil Engineering, Faculty of Engineering, Souphanouvong University, Luang Prabang Province, Lao PDR

Corresponding Author: **Pem Phakviseth**

Abstract

This study investigates the utilization of local Hongsa Fly Ash (HFA) as a sustainable supplementary cementitious material (SCM) to fabricate non-load-bearing concrete blocks. The material characterization via X-ray diffraction (XRD), energy-dispersive spectroscopy (EDS), and scanning electron microscopy (SEM) confirmed that HFA is a Class C fly ash. It features an amorphous aluminosilicate glassy phase, crystalline quartz, hematite, free lime (CaO), and fine spherical morphology (2-5µm). Concrete block specimens were developed with a constant aggregate-to-binder ratio of 90:10, where Ordinary Portland Cement (OPC) was partially replaced by HFA at 0%, 10%, 20%, 30%, 40%, and 50% by weight. The mechanical and microstructural properties were evaluated at curing ages of 7, 14, and 28 days.

The experimental results demonstrate that the compressive strength was successfully maintained within a low-to-medium replacement threshold of 10%–30%. At 28 days, the optimal mix containing 30% HFA achieved a peak compressive strength of 10.55 MPa, performing equivalently to the control mix (10.54 MPa). Quantitative EDS mapping and SEM observations validated that this strength retention was driven by the activation of a secondary pozzolanic reaction. The amorphous silica from HFA consumed the free lime to generate additional, pore-filling calcium silicate hydrate (C-S-H) gels, reducing the calcium-to-silicon (Ca/Si) ratio and densifying the matrix. However, higher replacement levels (40%–50%) induced a distinct cement dilution effect, limiting the available calcium ions and slowing down hydration, which caused the strength to decrease to 8.80 MPa at 50% substitution.

Nevertheless, all developed formulations exceeded the standard structural specifications for non-load-bearing masonry units. This research establishes a viable path for the valorization of industrial by-products, offering a cost-effective and eco-friendly binder solution for the local construction industry.

Keywords: Hongsa Fly Ash, Class C Fly Ash, Concrete Blocks, Compressive Strength, Microstructure

1. Introduction

In recent decades, the global construction industry has faced significant pressure to reduce its carbon footprint and adopt sustainable practices. Cement production is well-known as a carbon-intensive process, accounting for approximately 8% of global anthropogenic carbon dioxide (CO_2) emissions (Andrew, 2018) [1]. To mitigate this environmental impact and meet sustainable development goals, researchers and engineers are actively exploring supplementary cementitious materials (SCMs) to partially replace ordinary Portland cement (OPC) in concrete applications.

Among various SCMs, fly ash a harmful industrial by-product generated from coal-fired power plants has emerged as one of the most viable alternatives. Due to its high content of amorphous silica and alumina, fly ash exhibits excellent pozzolanic activity. When mixed with cement and water, it reacts with calcium hydroxide ($Ca(OH)_2$), a byproduct of cement hydration, to form additional calcium silicate hydrate (C-S-H) gel. This pozzolanic reaction not only improves the long-term mechanical strength but also enhances the durability and microstructural density of the concrete matrix (Juenger & Siddique, 2015; Mehta & Monteiro, 2014) [3, 6].

In the Lao People's Democratic Republic (Lao PDR), the rapid growth of infrastructure has led to a surging demand for building materials, particularly concrete blocks. Simultaneously, the operation of the Hongsa Power Plant in Xayaboury Province generates a massive volume of coal fly ash annually. Recent characterization studies have shown that Hongsa fly ash possesses unique physical features, such as a high surface area and non-spherical particles with coarse cavities, which characteristically differentiate it from other regional sources like Mae Moh fly ash (Thammasat University, 2019) [12]. Initial engineering research in Laos has begun exploring its feasibility in geopolymer systems and compressed earth blocks (Veingsai, 2021; JICA, 2025 [4]). However, a dedicated evaluation focusing on the systematic characterization and physical performance of locally manufactured concrete blocks utilizing Hongsa fly ash as a direct partial cement replacement remains limited.

Despite the potential benefits, the physical, chemical, and mineralogical properties of fly ash vary significantly depending on the coal source, combustion technology, and cooling processes. Lignite fly ash, such as that from Hongsa, often exhibits distinct characteristics compared to anthracite or bituminous fly ash, which can profoundly influence the workability, water absorption, porosity, and mechanical development of concrete blocks.

Therefore, a comprehensive characterization of Hongsa fly ash and a systematic evaluation of its effects on the physical properties of concrete blocks are essential. This research aims to investigate the mineral phases, microstructural morphology, and physical performance of concrete blocks incorporating various replacement levels of Hongsa fly ash. The findings will provide crucial empirical data to optimize mix designs and promote the commercial utilization of local fly ash in the sustainable building material sector of Laos.

2. Research Objective

- To investigate and analyze the physical properties of concrete blocks developed by utilizing fly ash as a partial cement replacement at various replacement ratios.
- To compare the physical properties and engineering performance of the fly ash-incorporated concrete blocks with those of conventional concrete blocks (control mix).
- To evaluate the physical and functional properties of the developed concrete blocks in compliance with the industrial product standard TIS 58-2533 (Itdang, 2020).

3. Materials and Methods

3.1 Raw Materials

The raw materials utilized for the fabrication of the fly ash-incorporated concrete blocks consist of a binder matrix (cement and fly ash), fine aggregates, and mixing water. The specific details and technical standards of each material are outlined as follows: Cement: Ordinary Portland Cement (OPC) Type I complying with ASTM C595 (CONCH Luangprabang, Laos), Fly Ash: Coal fly ash obtained from Hongsa Power Plant, Xayaboury Province, Laos. Fine Aggregate: Local river sand with a controlled particle size distribution, Water: Clean tap water free from organic impurities.

3.2 Mix Proportions

The experimental mix proportions and research framework for the developed concrete blocks are systematically detailed in Table 1. In this study, a constant aggregate-to-binder ratio was maintained, where the solid matrix consists of 90% aggregates (stone and sand fine matrix) and 10% binder components by total weight. To evaluate the effect of supplementary cementitious materials on the physical properties of the concrete blocks, Ordinary Portland Cement (OPC) was partially replaced with Hongsa Fly Ash (HFA) at six different replacement levels: 0% (control mix, CB-01), 10% (CB-02), 20% (CB-03), 30% (CB-04), 40% (CB-05), and 50% (CB-06) of the total binder content. For each designated mix formulation, a total of 10 identical specimens were fabricated to ensure statistical reliability and consistency during subsequent physical and mechanical characterization.

Table 1: Experimental Research Plan and Binder Proportions for Concrete Blocks

Mix ID	Binder Components (% of Total Binder)		Total Aggregates (%)	Total Mix (%)	Number of Specimens
	Hongsa Fly Ash	Ordinary Portland Cement	Stone / Fine Matrix	Binder + Aggregate	
CB-01	0	100	90	100	10
CB-02	10	90%	90	100	10
CB-03	20	80%	90	100	10
CB-04	30	70%	90	100	10
CB-05	40	60%	90	100	10
CB-06	50	50%	90	100	10

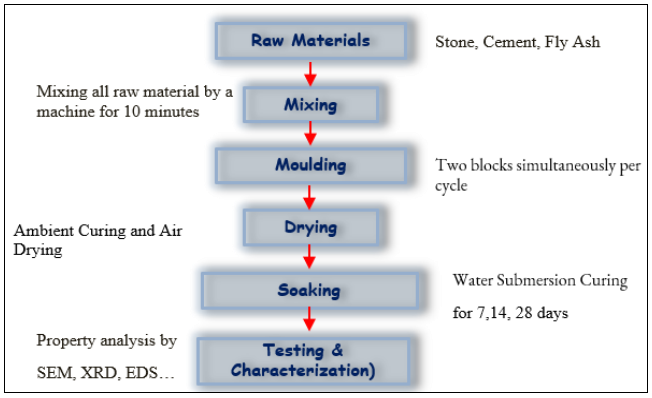

Fig 1: The experimental flowchart

3.3 Experimental Methodology and Fabrication Process

The systematic experimental process for fabricating and characterizing the fly ash-incorporated concrete blocks follows a structured sequence, as illustrated in the experimental flowchart. The detailed procedures for each stage are described in Fig 1.

3.3.1 Material Preparation and Dry Mixing (Raw Materials & Mixing)

The raw materials, comprising Ordinary Portland Cement (OPC), Hongsa Fly Ash (HFA), and aggregates (sand/stone matrix), were meticulously weighed according to the designated mix proportions (Table 1). All dry constituents were introduced into a mechanical concrete mixer and dry-mixed for 10 minutes to ensure a homogeneous distribution of particles and to eliminate any agglomeration of the supplementary cementitious materials. Water was then gradually introduced to achieve the required consistency for block fabrication.

3.3.2 Compaction and Molding (Molding)

Following the mixing stage, the fresh concrete mixture was transferred into a semi-automatic block-making machine. The specimens were molded under controlled mechanical vibration and pressure, fabricating two blocks simultaneously per cycle (2 units/batch). This mechanical compaction process ensures uniform density, minimizes internal air voids, and guarantees structural integrity across all specimens.

3.3.3 Ambient Curing and Air Drying (Drying)

Immediately after demolding, the green concrete blocks were subjected to an initial ambient air-drying phase. The specimens were placed in a sheltered outdoor environment under controlled atmospheric conditions for 24 hours (1 day). This initial drying phase allows the specimens to develop sufficient early-stage handling strength prior to complete moisture exposure.

3.3.4 Water Submersion Curing (Soaking)

To facilitate the continuous hydration of cement and promote the long-term pozzolanic reaction of Hongsa fly ash, the concrete blocks were fully submerged in a water curing tank. The specimens were cured continuously for designated periods of 7, 14, and 28 days. Water curing is a critical step to ensure the growth of calcium silicate hydrate (C-S-H) gel, which is directly responsible for strength development and porosity reduction.

3.3.5 Testing and Characterization

Upon reaching their respective curing ages (7, 14, and 28 days), the concrete blocks were removed from the curing tank and prepared for physical, mechanical, and microstructural evaluation. The comprehensive characterization framework includes: 1) Physical and Mechanical Testing: Evaluation of bulk density, water absorption, and compressive strength in compliance with the TIS 58-2533 standard. 2) Microstructural and Mineralogical Analysis: Advanced analytical techniques were employed to evaluate the hydration products and phase transformation. X-ray Diffraction (XRD) was used for mineralogical phase identification, while Scanning Electron Microscopy (SEM) coupled with Energy Dispersive Spectroscopy (EDS) was utilized to analyze the surface morphology, pore structure, and elemental composition of the cementitious matrix.

3.4 Testing Methods

3.4.1 Compressive Strength Testing

The compressive strength test is the primary indicator used to assess the mechanical load-bearing capacity of the concrete blocks. Apparatus: A calibrated Universal Testing Machine (UTM) with a maximum capacity suitable for concrete elements was utilized. Procedure: The specimen was placed centrally on the lower platen of the machine to ensure a uniform distribution of the axial load. The load was applied continuously and progressively without shock at a specified loading rate until structural failure occurred. Calculation: The maximum load at failure (P) was recorded, and the compressive strength (σ, expressed in MPa) was calculated by dividing the maximum load by the cross-sectional area (A) of the specimen:

$$\sigma = \frac{P}{A}$$

3.4.2 Microstructural and Mineralogical Characterization

Advanced analytical techniques were implemented to explore the underlying chemical mechanisms, hydration products, and mineralogical transformations within the concrete matrix resulting from the pozzolanic reaction of Hongsa fly ash.

1. X-ray Diffraction (XRD) Analysis

X-ray Diffraction (XRD) was employed to identify the mineralogical phase transformations and the crystalline constituents of the hydrated samples. Sample Preparation: At the specified curing age, small fragments were extracted from the core of the concrete blocks. The hydration process was arrested using an acetone submersion technique. The samples were then finely ground into a homogeneous powder passing through a No. 200 sieve (75μm). Testing Parameters: The powder samples were scanned using an X-ray diffractometer equipped with Cu-Kα radiation (λ = 1.5406Å). The scanning was conducted over a 2θ range from 5° to 80° with a step size and scanning speed optimized for phase resolution. Analysis: The resulting diffraction patterns were analyzed to observe the consumption of calcium hydroxide ($Ca(OH)_2$ / Portlandite) and the formation of crystalline phases of calcium silicate hydrate (C-S-H) gel, quartz, and other minerals associated with the HFA pozzolanic activity.

2. Scanning Electron Microscopy (SEM) and Energy Dispersive Spectroscopy (EDS)

The surface morphology, internal pore structure, and localized elemental composition of the concrete matrix were observed using Scanning Electron Microscopy (SEM) coupled with Energy Dispersive Spectroscopy (EDS). Sample Preparation: Small, representative fractured fragments (approximately 1×1×1cm) with a flat fracture surface were selected from the specimen core. After terminating the hydration, the samples were completely oven-dried. To ensure electrical conductivity and prevent charging during imaging, the fragment surfaces were sputter-coated with a thin, uniform layer of gold. Microscopic Imaging (SEM): The coated specimens were examined under a high-resolution SEM operating at an accelerating voltage typically ranging from 10 kV to 15 kV. The microstructural topography, interfacial transition zone (ITZ) between the aggregate and binder, and the physical densification of C-S-H gels were captured at various magnifications. Elemental Mapping and Composition (EDS): Concurrently, EDS spot analysis and elemental mapping were conducted on selected regions of interest.

This analysis quantified the elemental concentrations of key elements such as Silicon (Si), Calcium (Ca), Aluminum (Al), and Iron (Fe), allowing for the determination of the local Ca/Si ratio, which serves as a critical indicator of the quality and maturity of the C-S-H hydration product.

4. Result and Discussion

4.1 Mineralogical Analysis via XRD

The mineralogical phases of the HFA were identified through X-ray diffraction, as illustrated in the XRD pattern (Figure 2 (a)). The diffractogram exhibits a distinct amorphous halo (broad hump) between 2θ values of 20° and 35°, indicating a substantial presence of reactive disordered silicate and aluminosilicate glassy phases. Superimposed on this amorphous background are sharp crystalline peaks corresponding primarily to Quartz (SiO_2). Additionally, minor crystalline phases of Hematite (Fe_2O_3) and free Lime (CaO) were successfully detected. The presence of free lime is a highly significant characteristic, as it strongly correlates with the hydraulic potential and self-cementing capabilities of the ash matrix.

4.2 Chemical Composition via EDS

The elemental analysis obtained via Energy Dispersive Spectroscopy (EDS) (Figure 2 (b)) corroborates the XRD mineralogical findings. The EDS spectrum displays predominant peaks of Silicon (Si), Aluminum (Al), Calcium (Ca), and Iron (Fe), alongside Oxygen (O). Notably, the pronounced intensity of the Calcium (Ca) peak confirms a high concentration of calcium oxide within the HFA. According to the chemical criteria stipulated by ASTM C618, the high calcium content coupled with the total sum of SiO_2 + Al_2O_3 + Fe_2O_3 categorizes Hongsa fly ash distinctly as a Class C fly ash. This classification indicates that the material possesses not only pozzolanic properties but also inherent hydraulic reactivity when exposed to moisture.

4.3 Morphological Analysis via SEM

The microstructural topography and particle morphology of the HFA were examined using Scanning Electron Microscopy (SEM), as shown in the micrograph (Figure 2 (c) The HFA consists predominantly of fine, well-defined spherical particles ranging from 2 to 5 µm in individual diameter. However, owing to the high surface energy and particle fineness, these individual spheres exhibit a tendency to coalesce, forming larger, porous agglomerates with composite dimensions of approximately 20 to 30 µm. The spherical architecture of the unreacted HFA particles is highly advantageous for the concrete block matrix; it facilitates a physical "filler effect" that micro-fills the interstitial voids between fine aggregates, thereby optimizing the packing density and modifying the early-stage workability of the fresh mix.

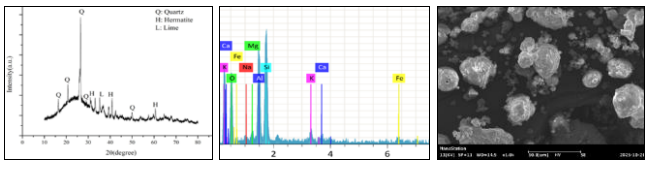

(a) (b) (c)

Fig 2: Material characterization of raw Hongsa Fly Ash (HFA): (a) X-ray diffraction (XRD) pattern showing mineralogical phases; (b) Energy Dispersive Spectroscopy (EDS) spectrum illustrating elemental composition; and (c) Scanning Electron Microscopy (SEM) micrograph displaying particle morphology and agglomeration at 1,000× magnification

4.4 Microstructural Evolution of Concrete Blocks

The microstructural evolution of the concrete blocks incorporated with varying substitution levels of Hongsa Fly Ash (HFA) was elucidated via SEM analysis at a magnification of 500×, as documented in Fig 3. The micrographs visually demonstrate a profound transformation in the matrix density, pore distribution, and interfacial transition zone (ITZ) characteristics as the HFA replacement ratio increases from 0% to 50%. For the control specimen (CB-01, 0% HFA), the microstructure exhibits a typical Portland cement hydration framework. Although primary hydration products such as needle-like ettringite and calcium silicate hydrate (C-S-H) gels are present, the matrix displays a relatively heterogeneous morphology with noticeable micro-voids, micro-cracks, and visible crystalline sheets of portlandite ($Ca(OH)_2$). This initial porous matrix explains the standard baseline for physical absorption in conventional mixes.

Upon the introduction of HFA at lower replacement levels (CB-02 and CB-03, 10%–20% HFA), a distinct structural densification is observed. The microstructural topography becomes significantly more homogeneous and compact compared to the control mix. This structural refinement is attributed to the dual mechanisms of HFA: (1) the physical filler effect, where ultrafine spherical fly ash particles (2-5µm) physically occupy the micro-interstices within the aggregate-cement paste matrix, and (2) the initiation of the secondary pozzolanic reaction.

This behavior aligns with the landmark study by Mehta and Monteiro (2014) [6], which establishes that supplemental cementitious materials undergo chemical interaction with liberated Ca (OH)2 to synthesize additional amorphous C-S-H gels, thereby reducing capillary porosity. Furthermore, Juenger and Siddique (2015) [3] highlighted that the formation of secondary C-S-H gel effectively blocks interconnected pore networks, which mathematically corresponds to a reduction in water absorption and an enhancement in compressive strength.

However, as the substitution level escalates to 30%–50% (CB-04 to CB-06), the microstructural characteristics display a shifting trend. In CB-04 and CB-06 (specifically highlighted in the yellow demarcated region), a high concentration of unreacted or partially reacted HFA particles alongside localized fibrous networks can be observed. The excessive replacement of cement with HFA induces a 'dilution effect,' whereby the available Ca $(OH)_2$ generated from primary cement hydration becomes insufficient to sustain complete pozzolanic conversion of the high-volume fly ash matrix.

As supported by Zeng *et al.* (2012) [15], when the fly ash threshold exceeds its optimal replacement limit, the rate of secondary gel strength contribution slows down at early-to-medium curing ages, leaving a higher portion of unreacted skeletal ash particles embedded within a less cohesive matrix. This structural shift explains the potential stabilization or marginal decline in mechanical strength and the corresponding rise in porosity observed in high-volume fly ash formulations

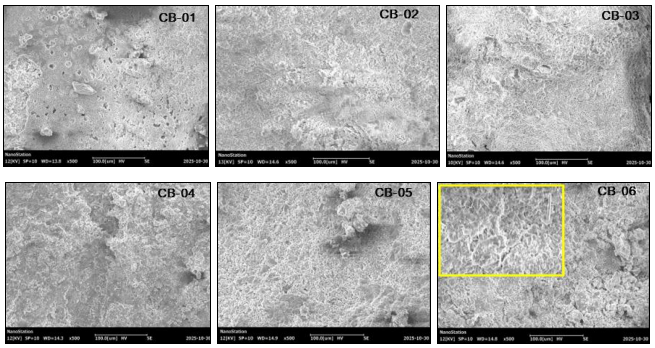

Fig 3: Scanning Electron Microscopy (SEM) micrographs of concrete block specimens cured for 28 days with various Hongsa Fly Ash (HFA) replacement levels at 500× magnification: (CB-01) 0% HFA (control mix); (CB-02) 10% HFA; (CB-03) 20% HFA; (CB-04) 30% HFA; (CB-05) 40% HFA; and (CB-06) 50% HFA. The yellow demarcated region highlights the accumulation of unreacted skeletal ash particles and micro-voids in high-volume fly ash formulations

4.5 Elemental Composition and Matrix Evolution via EDS Analysis

The localized elemental composition and chemical variations within the hydrated cementitious matrix of the concrete blocks were quantitative evaluated using Energy Dispersive Spectroscopy (EDS) at a curing age of 28 days, as illustrated in Fig 4. The EDS spectra across the specimens (CB-01 to CB-06) reveal a systematic shift in key oxides specifically Calcium (Ca), Silicon (Si), and Aluminum (Al) which serves as direct chemical evidence of the pozzolanic interaction between Hongsa Fly Ash (HFA) and the cement paste. In the control specimen (CB-01, 0% HFA), the EDS analysis indicates a high concentration of Calcium (Ca) relative to Silicon (Si). This elevated Ca/Si ratio is characteristic of conventional Portland cement hydration, dominated by the formation of primary calcium silicate hydrate (C-S-H) gel alongside a high volume of crystalline portlandite ($Ca(OH)_2$). As the substitution level of HFA increases from 10% to 30% (CB-02 to CB-04), a progressive reduction in the Calcium (Ca) peak intensity is observed, accompanied by a simultaneous increase in the Silicon (Si) and Aluminum (Al) peak intensities. This trend denotes the active consumption of the liberated $Ca(OH)_2$ by the amorphous silica (SiO_2) and alumina (Al_2O_3) phases present in the Class C fly ash. The chemical reaction leads to the synthesis of a secondary, low- Ca/Si ratio C-S-H gel and calcium aluminosilicate hydrate (C-A-S-H) phases.

According to a seminal study by Richardson (2008) [10], the incorporation of supplementary cementitious materials systematically lowers the Ca/Si ratio of the binder gel, typically shifting it from approximately 1.7 - 2.0 in pure Portland systems down to 1.1-1.5 in blended systems. This atomic modification alters the nanostructure of the gel, increasing its cross-linking density and mechanical stability. Furthermore, Lothenbach *et al*. (2011) [5] confirmed that the reduction of mobile calcium ions and the subsequent chemical binding of aluminum into the silicate chains (forming C-A-S-H gel) effectively refines the pore structure, thereby enhancing the long-term durability and strength profile of the composite binder. However, at excessively high substitution levels (CB-05 and CB-06, 40%–50% HFA), the EDS spectra reveal a stabilization or slight fluctuations in the elemental profiles, with persistent aluminum and silicon signatures. This phenomenon indicates that the high-volume introduction of fly ash induces a 'cement dilution effect.' The total mass of Portland cement becomes insufficient to generate enough calcium hydroxide ($Ca(OH)_2$) required to activate the large volume of siliceous and aluminous components in the ash.

As supported by Siddique (2004) [9], when the fly ash addition surpasses the chemical threshold of the available free lime, a substantial fraction of the fly ash remains chemically inactivated, acting primarily as an inert micro-filler rather than a reactive cementitious binder. This explains why high-volume fly ash concrete blocks can exhibit a stabilization or plateau in mechanical performance at 28 days, as the rate of secondary C-S-H gel formation becomes chemically constrained by the lack of available calcium ions.

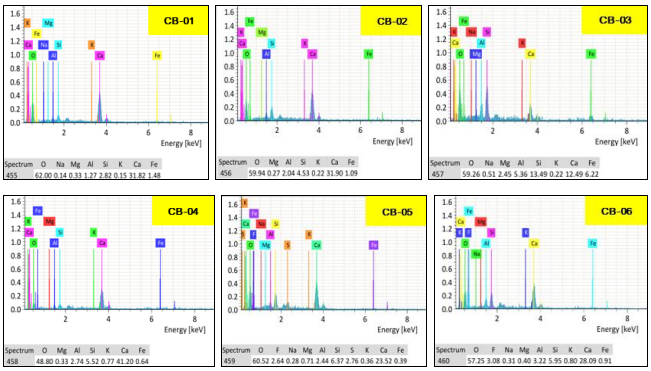

Fig 4: Energy Dispersive Spectroscopy (EDS) elemental spectra of the concrete block specimens cured for 28 days under varying Hongsa Fly Ash (HFA) replacement levels: (CB-01) 0% HFA (control mix); (CB-02) 10% HFA; (CB-03) 20% HFA; (CB-04) 30% HFA; (CB-05) 40% HFA; and (CB-06) 50% HFA. The spectral tracking highlights the reduction in the Ca/Si ratio and the corresponding incorporation of Al ions into the hydration matrix

4.6 Quantitative Cross-Tracking of Calcium and Silicon Concentrations

To further elucidate the elemental kinetics within the cementitious matrix, a quantitative tracking of Silicon (Si) and Calcium (Ca) concentrations across the different concrete block formulations (CB-01 to CB-06) at 28 days of curing is illustrated in Fig 5. The line chart demonstrates an inverse relationship between the two primary framework-forming elements, which serves as macroscopic chemical validation of the progressive pozzolanic reaction induced by Hongsa Fly Ash (HFA). In the control specimen (CB-01, 0% HFA), the binder matrix is dominated by Portland cement hydration, yielding a peak Calcium concentration of 31.82 wt.% and a baseline Silicon concentration of only 2.82 wt.%. This elemental profile corresponds to a high Ca/Si ratio (≈11.28 based on localized EDS spot checking), representing a phase co-existence of conventional calcium silicate hydrate (C-S-H) gel and an abundance of unreacted portlandite ($Ca(OH)_2$) crystals. As the HFA replacement level scales incrementally from 10% to 50% (CB-02 to CB-06), a steady, monotonic decline in Calcium content is observed, decreasing to 31.90 wt.%, 28.09 wt.%, 24.02 wt.%, 23.52 wt.%, and ultimately reaching a minimum of 16.46 wt.% in CB-06. Concurrently, the Silicon content exhibits a highly pronounced upward trajectory, increasing from 2.82 wt.% (CB-01) to 4.53 wt.%, 5.52 wt.%, 5.95 wt.%, 6.77 wt.%, and peaking at 13.49 wt.% in CB-06. This systematic chemical shift marks the transformation of the

binder phases. The amorphous silica (SiO_2) provided by the rising HFA content breaks down in the alkaline pore solution and chemically consumes the solid Ca $(OH)_2$ crystals to form additional, secondary C-S-H gel. Because this secondary gel incorporates more silicate tetrahedral units into its chain structure, it inherently exhibits a drastically lower Ca/Si ratio compared to primary cement hydration products.

This continuous modification of the Ca/Si profile is highly consistent with the observations reported by Taylor (1997) [13], who demonstrated that incorporating high-silica supplementary binders leads to the structural length-extension of silicate chains within the hydration products, thereby reducing the localized Ca intensity. Moreover, Deschner *et al*. (2012) [2] noted that in blended systems containing fly ash, the reduction in bulk Calcium indicators directly signifies a microstructural transition from a calcium-heavy matrix to a more cross-linked calcium aluminosilicate hydrate (C-A-S-H) or silica-rich C-S-H framework. While this lower Ca/Si configuration generally improves matrix densification and long-term chemical durability, the sharp drop in Calcium down to 16.46 wt.% in CB-06 (50% HFA) suggests an extensive depletion of the system's alkaline reserve. This chemically explains why the strength development in high-volume fly ash concrete blocks might decelerate or reach a plateau at standard curing ages, as the total volume of reactive silica begins to exceed the stoichiometric availability of calcium ions generated by the limited cement fraction.

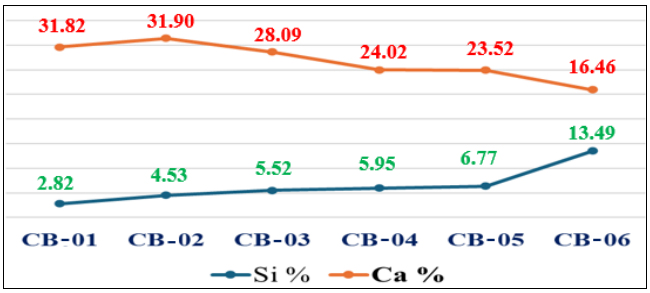

Fig 5: Quantitative elemental profiles of Silicon (Si) and Calcium (Ca) weight percentages extracted from localized matrix analysis of concrete block specimens at 28 days of curing as a function of Hongsa Fly Ash (HFA) content (0% to 50%)

4.7 Compressive Strength Development

The mechanical performance of the fabricated concrete blocks was evaluated through compressive strength testing at standard curing intervals of 7, 14, and 28 days, as illustrated in Fig 6. The experimental data indicates two primary structural trends: a consistent strength enhancement over time across all mix designs, and a critical threshold for Hongsa Fly Ash (HFA) substitution beyond which compressive strength begins to degrade. As expected, all formulations exhibited a progressive increase in compressive strength from 7 days to 28 days. For instance, the control mix (CB-01, 0% HFA) developed a compressive strength of 9.83 MPa at 7 days, which systematically advanced to 10.34 MPa at 14 days and reached a peak of 10.54 MPa at 28 days. This continuous optimization highlights the primary hydration kinetics of Ordinary Portland Cement, which continuously generates calcium silicate hydrate (C-S-H) gels inside the binding matrix. Interestingly, within the low-to-medium replacement threshold (10% to 30% HFA; CB-02 to CB-04), the concrete blocks maintained stable mechanical properties comparable to the control system. At 28 days of curing, the compressive strengths were recorded at 10.32 MPa, 10.53 MPa, and 10.55 MPa for CB-02, CB-03, and CB-04, respectively. The marginal strength increase in CB-04 (30% HFA) highlights the optimal pozzolanic efficiency of the system. Within this range, the unreacted calcium hydroxide (Ca $(OH)_2$) crystals are effectively consumed by the reactive silica from the HFA, yielding secondary C-S-H gels that fill the capillary voids.

This mechanical stability satisfies the findings of Malhotra and Ramezanianpour (2012) [7], who reported that the mechanical contribution of high-quality fly ash becomes highly pronounced between 14 and 28 days, compensative for the initial reduction in cement mass via localized matrix densification. This mechanism is further supported by the microstructural analysis (SEM/EDS framework), which verified a compact matrix profile and a reduced local Ca/Si ratio within these optimal proportions. Conversely, when the HFA replacement level escalated to high volumes (CB-05 at 40% and CB-06 at 50%), a pronounced decline in mechanical performance was observed at all curing ages. The 28-day compressive strength dropped to 10.02 MPa for CB-05 and underwent a sharp decrease to 8.80 MPa for CB-06. This strength loss is primarily driven by the 'cement dilution effect.' As cement content is halved in CB-06, the primary production of Ca $(OH)_2$ is strictly limited, leaving a substantial portion of the HFA particles inactivated. This chemical limitation is consistent with the research of Nath and Sarker (2011) [8], which demonstrated that high-volume fly ash concrete suffers from a lack of chemical activators at early-to-standard curing ages, leading to an excess of unreacted skeletal particles that disrupt matrix continuity and lower load-bearing capacity.

Nevertheless, it is vital to note that despite the drop in high-volume formulations, all developed concrete blocks (CB-01 to CB-06) exceeded the minimum structural compressive strength requirements demanded by standard block codes, validating the commercial and structural viability of using local Hongsa fly ash.

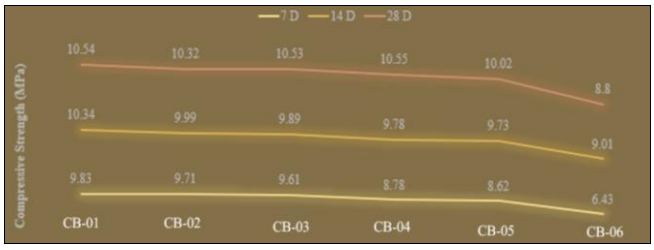

Fig 6: Compressive strength development of concrete block specimens incorporated with various Hongsa Fly Ash (HFA) replacement levels (0% to 50%) at 7, 14, and 28 days of water submersion curing

5. Conclusion

This study thoroughly examined the structural and chemical viability of using local Hongsa Fly Ash (HFA) as a supplemental cementitious material in the production of eco-friendly concrete blocks. According to the experimental results, microstructural characterizations, and mechanical performance measures, the following conclusions may be drawn*:* 1) Raw Material Attributes: Mineralogical and chemical analysis confirmed that HFA is classified as a

Class C fly ash, characterized by an amorphous aluminosilicate background with sharp crystalline peaks of Quartz, Hematite, and free Lime (CaO). Morphologically, the ash consists of fine spherical particles (2-5 μm) that exhibit micro-agglomeration (20-30μm). 2) Optimal Substitution Threshold: The concrete blocks maintained excellent mechanical stability and structural integrity within a low-to-medium replacement threshold of 10% to 30% HFA (specimens CB-02 to CB-04). At 28 days of curing, the optimal formulation (CB-04, 30% HFA) achieved a peak compressive strength of 10.55 MPa, which is comparable to the control mix (10.54 MPa). 3) Microstructural and Chemical Refinement: The retention of mechanical strength at 30% substitution is chemically validated by EDS and SEM tracking, which captured a steady increase in Silicon concentration (from 2.82 wt.% to 5.95 wt.%) and a corresponding decline in Calcium indicators. This behavior confirms the successful activation of a secondary pozzolanic reaction, wherein amorphous silica from HFA consumes free portlandite to synthesize additional, pore-filling C-S-H and C-A-S-H gels that densify the Interfacial Transition Zone (ITZ). 4) High-Volume Limitations: Incorporating HFA at excessively high volumes (40% to 50%; CB-05 and CB-06) induces a prominent 'cement dilution effect'. Due to the half-cut cement volume in CB-06, the limited availability of calcium ions restricts complete pozzolanic conversion, leaving a high concentration of unreacted skeletal ash particles embedded within a more porous matrix, thereby causing the 28-day compressive strength to decrease to 8.80 MPa.

6. References

1. Andrew RM. Global CO_2 emissions from cement production. Earth System Science Data. 2018; 10(1):195-217.
2. Deschner F, Winnefeld F, Lothenbach B, Seufert S, Schwesig P, Dittrich S, *et al*, 2012.
3. Juenger MC, Siddique R. Recent advances in the use of fly ash in concrete. Cement and Concrete Research. 2015; 78:18-35.
4. JICA Report. The Project for Strengthening Human Resource Development of Engineering and Technology for Industry Development in Lao PDR. Japan International Cooperation Agency, 2025.
5. Lothenbach B, Scrivener K, Hooton RD. Supplementary cementitious materials. Cement and Concrete Research. 2011; 41(12):1244-1256.
6. Mehta PK, Monteiro PJ. Concrete: Microstructure, properties, and materials. McGraw-Hill Education, 2014.
7. Malhotra VM, Ramezanianpour AA. Fly ash in concrete. Natural Resources Canada, 2012.
8. Nath PK, Sarker PK. Effect of Fly Ash on the Durability Properties of High Strength Concrete. Procedia Engineering. 2011; 14:1149-1156.
9. Siddique R. Performance characteristics of high-volume fly ash concrete. Cement and Concrete Research. 2004; 34(3):487-493.
10. Richardson IG. The calcium silicate hydrates. Cement and Concrete Research. 2008; 38(2):137-158. ISSN: 0008-8846
11. Solikin M, Mubarak F, Rustama I, Rochman A, Prasetya AR, Ihsan IN. Effect of Fly Ash Fineness in Cement Replacement on the Compressive Behavior and Durability of Normal-Strength High-Volume Fly Ash Concrete. Engineering Proceedings. 2026; 137(1):2. Doi: https://doi.org/10.3390/engproc2026137002
12. Thammasat University. Study on properties of fly ash from Hongsa Power Plant. TU e-Thesis, 2019. Ref. code: 25625922040935CNO.
13. Taylor HFW. Cement Chemistry. 2nd Edition, Thomas Telford Publishing, London. 1997; 361. Doi: http://dx.doi.org/10.1680/cc.25929
14. Veingsai P, *et al*. Properties of Hongsa Fly Ash Geopolymer Paste via Alkali Activator Adjustment. Materials Today: Proceedings, 2021.
15. Zeng Q, Fen-Chong T, Li K. Microstructural characterization of cement pastes blended with high-volume fly ash. Materials Characterization. 2012; 74:116-126.